BRAIN
A JOURNAL OF NEUROLOGY

Stimulation of autophagy reduces neurodegeneration in a mouse model of human tauopathy

Véronique Schaeffer,[1] Isabelle Lavenir,[1] Sefika Ozcelik,[2,3] Markus Tolnay,[3] David T. Winkler[2,3] and Michel Goedert[1]

1 MRC Laboratory of Molecular Biology, Cambridge CB2 0QH, UK
2 Department of Neurology, University Hospital Basel, CH-4031 Basel, Switzerland
3 Institute of Pathology, University Hospital Basel, CH-4031 Basel, Switzerland

Correspondence to: Michel Goedert,
Medical Research Council Laboratory of Molecular Biology,
Hills Road, Cambridge CB2 0QH,
UK
E-mail: mg@mrc-lmb.cam.ac.uk

The accumulation of insoluble proteins is a pathological hallmark of several neurodegenerative disorders. Tauopathies are caused by the dysfunction and aggregation of tau protein and an impairment of cellular protein degradation pathways may contribute to their pathogenesis. Thus, a deficiency in autophagy can cause neurodegeneration, while activation of autophagy is protective against some proteinopathies. Little is known about the role of autophagy in animal models of human tauopathy. In the present report, we assessed the effects of autophagy stimulation by trehalose in a transgenic mouse model of tauopathy, the human mutant P301S tau mouse, using biochemical and immunohistochemical analyses. Neuronal survival was evaluated by stereology. Autophagy was activated in the brain, where the number of neurons containing tau inclusions was significantly reduced, as was the amount of insoluble tau protein. This reduction in tau aggregates was associated with improved neuronal survival in the cerebral cortex and the brainstem. We also observed a decrease of p62 protein, suggesting that it may contribute to the removal of tau inclusions. Trehalose failed to activate autophagy in the spinal cord, where it had no impact on the level of sarkosyl-insoluble tau. Accordingly, trehalose had no effect on the motor impairment of human mutant P301S tau transgenic mice. Our findings provide direct evidence in favour of the degradation of tau aggregates by autophagy. Activation of autophagy may be worth investigating in the context of therapies for human tauopathies.

Introduction

Most neurodegenerative diseases are characterized by the accumulation of misfolded proteins. Thus, α-synuclein aggregates in Parkinson's disease and other synucleinopathies, TDP-43 (TAR DNA-binding protein 43) in TDP-43 proteinopathies, huntingtin in Huntington's disease and both β-amyloid and tau in Alzheimer's disease (Goedert et al., 2010). Filaments made of hyperphosphorylated tau protein are a good predictor of the cognitive state in Alzheimer's disease, because a negative correlation has been described between the number of neurofibrillary tangles, and the Mini-Mental score (Giannakopoulos et al., 2003).

Tau deposits also constitute the defining pathological hallmark of several other diseases, including progressive supranuclear palsy, corticobasal degeneration, Pick's disease and frontotemporal dementia and parkinsonism linked to chromosome 17 (Goedert and Jakes, 2005; Goedert and Spillantini, 2011). Since filament assembly is a concentration-dependent process, a reduction in the production and/or increased clearance of tau are potential targets.

In eukaryotic cells, there are two major systems responsible for the degradation of cytoplasmic proteins: the ubiquitin–proteasome system and the autophagy–lysosome pathway (Goldberg, 2003). The accumulation of ubiquitinated tau in intracellular filamentous inclusions suggests a possible impairment of tau degradation by the ubiquitin–proteasome system and/or the autophagy–lysosome pathway. Indeed, inactivation of the ubiquitin–proteasome system or the autophagy–lysosome pathway has been reported to lead to neurodegeneration associated with the presence of ubiquitinated aggregates (Hara *et al.*, 2006; Komatsu *et al.*, 2006; Bedford *et al.*, 2008; Riley *et al.*, 2010). Particularly, ubiquitin–proteasome system or autophagy–lysosome pathway inhibition induces the accumulation of tau (Blard *et al.*, 2006; Ramesh Babu *et al.*, 2008; Liu *et al.*, 2009; Lee *et al.*, 2010). Moreover, accumulation of autophagic vacuoles has been observed in Alzheimer's disease brain and in a mouse model of tauopathy (Lin *et al.*, 2003; Nixon *et al.*, 2005), suggesting a possible disturbance of lysosomal proteolysis in tauopathy. Macroautophagy (hereafter referred to as autophagy) is the major form of autophagy. Although it is known that the suppression of autophagy causes neurodegeneration (Hara *et al.*, 2006), relatively little is known about the role of autophagy in animal models of human tauopathy. In the triple transgenic mouse model of Alzheimer's disease and in a mouse model expressing human mutant tau on a null background for the E3 ubiquitin ligase parkin, stimulation of autophagy promoted the degradation of insoluble tau (Caccamo *et al.*, 2011; Majumder *et al.*, 2011; Rodriguez-Navarro *et al.*, 2011). However, these studies did not allow one to determine whether the effects of autophagy stimulation were due to a direct interaction between the autophagic machinery and tau or whether they were indirect. To date, there has been no report of the effect of increased autophagy in a mouse model of human tauopathy. We therefore administered trehalose, a mammalian target of rapamycin (mTOR)-independent activator of autophagy (Noda and Ohsumi, 1998; Sarkar *et al.*, 2007a), to mice transgenic for human mutant P301S tau.

Materials and methods

Antibodies

We used phosphorylation-independent anti-tau antibodies BR133 and BR134 which recognize both murine and human tau isoforms. Phosphorylation-dependent anti-tau antibodies AT8 and AT100 (Innogenetics) were also used. AT8 recognizes tau protein phosphorylated at S202 and T205 (Goedert *et al.*, 1995), whereas AT100 detects tau phosphorylated at T212, S214 and T217 (Yoshida and Goedert, 2006). Autophagy was assessed using an antibody against

microtubule-associated protein light chain 3 (LC3) (Novus Biologicals). We also used an antibody against p62/SQSTM1 (Santa Cruz Biotechnology). To normalize protein levels, an anti-GAPDH (Millipore, Ltd.) antibody was used.

Animals and treatment

Homozygous human P301S tau transgenic mice (Allen *et al.*, 2002) and age-matched wild-type C57BL/6 mice were used ($n = 6$ per group for western blot analysis; $n = 3$ per group for immunohistochemistry and stereology experiments). From weaning onwards, the animals were treated with 2% trehalose or 2% sucrose, which were used as the control. A separate group received normal drinking water (no treatment). The water solutions were changed twice weekly. Animals were checked daily and the quantity of water drunk and the animals' weights were assessed twice a week. P301S tau transgenic mice develop motor deficits at ∼3–4 months of age, as shown using Rotarod (Scattoni *et al.*, 2010). We routinely evaluated these deficits by visual inspection, as they form in a stereotypical manner consisting of an unstable gait followed by general stiffness and hindlimb paralysis. Furthermore, at 3–4 months of age, the human P301S tau mice are unable to extend their hindlimbs when lifted by the tail (Allen *et al.*, 2002). In this study, we assessed the motor deficits by visual inspection and used the time when all the animals had developed hindleg stiffness and were unable to extend their hindlimbs when suspended by the tail as the endpoint (20 weeks of age).

Tissue extraction

To extract sarkosyl-insoluble proteins from brain and spinal cord, frozen tissues were weighed and homogenized in cold extraction buffer [10 mM Tris–HCl, pH 7.4, 800 mM NaCl, 1 mM EGTA, 0.1 M phenylmethylsulphonyl fluoride, 10% sucrose and one tablet of complete protease inhibitor cocktail (Roche)]. The homogenates were spun at $6000g$ for 20 min and the supernatants incubated with 1% sarkosyl for 1 h at room temperature. After a 1 h centrifugation at $80\,000g$, the supernatants were discarded and the pellets resuspended in 50 mM Tris–HCl, pH 7.4 (300 µl/g tissue). For investigation of soluble tau, brains and spinal cords were homogenized in 25 mM Tris–HCl, pH 7.4, 150 mM NaCl, 1 mM EDTA, 1 mM EGTA, 1 mM phenylmethylsulphonyl fluoride and one tablet of complete protease inhibitor cocktail. Samples were centrifuged at $80\,000g$ for 15 min. The resulting supernatant constituted the soluble fraction. The samples were analysed by SDS-PAGE.

Immunoblot analysis

After SDS-PAGE, the gels were blotted for 1 h at room temperature onto polyvinylidene difluoride membranes (Millipore). The membranes were blocked for 1 h at room temperature in 0.1 M phosphate buffer, pH 7.4, 0.2% Tween 20 and 5% milk, followed by an overnight incubation with the primary antibody in blocking buffer. Membranes were then washed in 0.1 M phosphate buffer, pH 7.4, 0.2% Tween 20 and incubated for 1 h at room temperature with peroxidase-conjugated secondary antibody (Pierce) in blocking solution. After washing, the blots were developed using enhanced chemiluminescence (Amersham Biosciences).

Quantification of proteins

Band intensities were quantified (Chemidoc™ XRS and Quantity One® software, Bio-Rad) and the amounts of soluble proteins normalized with respect to GAPDH. Insoluble tau was normalized relative to the tissue weight. Data were expressed as means ± SEM. Statistical analysis was performed using a one-way ANOVA test followed by Tukey's *post hoc* comparisons (Prism, GraphPad Software, Inc.).

Immunohistochemistry

Mice were perfused transcardially with 4% paraformaldehyde in 0.1 M phosphate buffer, pH 7.4. Brains and spinal cords were dissected and post-fixed overnight at 4°C, followed by cryoprotection in PBS containing 30% sucrose for at least 24 h. Serial sagittal brain sections (30 μm) were cut on a Leica SM2400 microtome (Leica Microsystems) and stored at 4°C in PBS containing 0.1% sodium azide. For fluorescence labelling, sections were permeabilized for 5 min with cold PBS containing 0.5% Triton X-100 and washed three times with PBS, 0.1% Triton X-100 (PBST). After 2 h blocking at room temperature with PBST containing 3% bovine serum albumin, sections were incubated with the primary antibodies in blocking solution for 24 h at 4°C. This was followed by three washes and a 2 h incubation at room temperature with Alexa Fluor® 488 (Molecular Probes) or Cy5 (Abcam) secondary antibodies in blocking solution. After washing and DAPI (4,6-diamidino-2-phenylindole) staining, the sections were mounted using Vectashield mounting medium (Vector Laboratories). They were analysed using a Leica DMRB fluorescence microscope (Leica) or a Radiance 2100 confocal microscope (Bio-Rad). Images were taken using a Sharp 2000 laser (Zeiss Bio-Rad) and were typically 512×512 pixels. Staining for neuronal nuclei (NeuN; Chemicon) (Mullen *et al.*, 1992; Wolf *et al.*, 1996; Lind *et al.*, 2005) and tau phosphorylated at the AT100 epitope were carried out in brains of wild-type and transgenic mice using immunoperoxidase (Vectastain ABC kit, Vector Laboratories). Endogenous peroxidase was quenched for 15 min with 3% H_2O_2 in distilled water. After washing, sections were blocked for 1 h with normal horse serum in PBST and incubated overnight with the anti-NeuN antibody (1:500) in blocking solution at 4°C. After three rinses with PBST, sections were incubated with a biotin-conjugated anti-mouse antibody for 2 h at room temperature. Next, the avidin–biotin-conjugated complex was applied for a further 2 h. Finally, the antigen was visualized using the Vector® VIP substrate kit (Vector Laboratories). Sections were mounted on SuperFrost® glass slides (VWR international) and dehydrated using a series of ascending ethanol solutions (70, 95 and 100%) and xylene.

Stereology

The Stereo Investigator 9 (MBF Bioscience) was used to quantify the number of NeuN-positive cells. Sections through the brain were sampled in a systematic random manner using 1:12 series for quantification of NeuN-positive and AT100-positive neurons. The thickness of each section was determined using the Stereo Investigator 9 software. For a given section, the outline of the region of interest was traced under a ×10 objective and the enclosed area calculated by the software. Sections within the highlighted area were then sampled at random and cells counted under the ×40 objective to determine the total number of immunoreactive cells. Statistical analyses were performed using a one-way ANOVA test followed by Tukey's *post hoc* comparisons (Prism, GraphPad Software, Inc.).
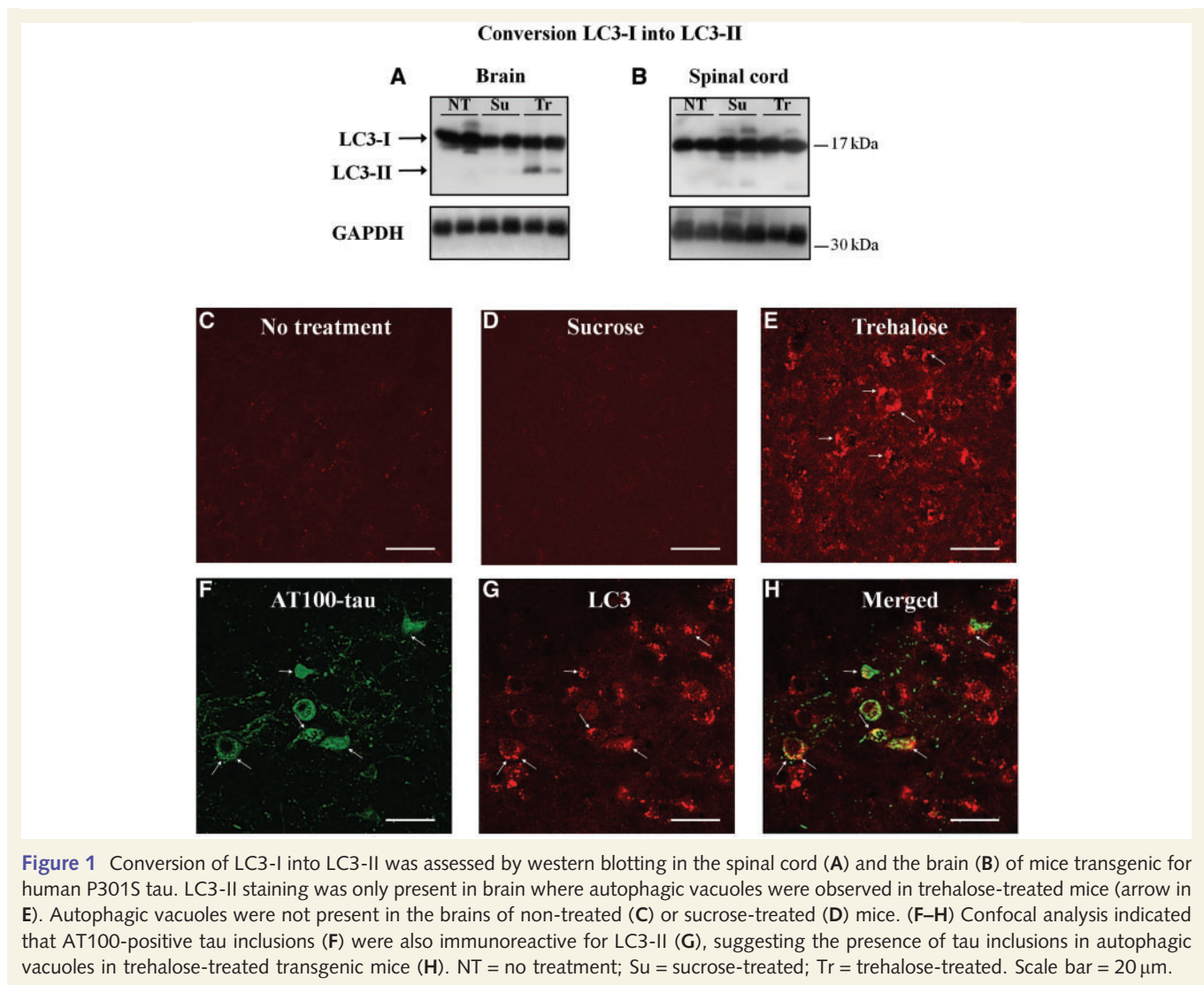
Results

Animal health

Water consumption of the three groups (no treatment, sucrose-treated and trehalose-treated) was similar. Sucrose and trehalose had no impact on the animals' weights or coat aspects, suggesting that the health of the mice was similar among the three groups. The human P301S tau mice were sacrificed at 20 weeks of age, when they developed an unstable gait and motor abnormalities, which is typical of homozygous transgenic mice (Allen *et al.*, 2002). The development of motor deficits was not significantly different between treated and non-treated human P301S tau transgenic mice. Thus, untreated mice developed the first motor deficits at 19 ± 0.19 weeks of age, which was not significantly different from the ages at which they appeared in sucrose-treated (18.8 ± 0.31 weeks) and trehalose-treated (19.25 ± 0.23 weeks) mice (Supplementary Fig. 1).

Effects of trehalose on autophagy activation

To investigate autophagy activation, we measured the conversion of LC3-I into LC3-II, a marker of autophagic vacuole formation (Kabeya *et al.*, 2000; Mizushima *et al.*, 2004; Tanida *et al.*, 2004). We observed the conversion of $17.5 \pm 2.3\%$ LC3-I into LC3-II in the brains of trehalose-treated mice, while no detectable LC3-I conversion was seen in untreated or sucrose-treated mice (Fig. 1A). Unexpectedly, trehalose had no effect on LC3-I conversion in the spinal cord (Fig. 1B). We therefore focused our study on the brain. Immunohistochemistry of brain sections from mice transgenic for human mutant P301S tau showed the presence of LC3 puncta in trehalose-treated mice (Fig. 1E). The punctate distribution of LC3 was absent from control groups (Fig. 1C and D). In trehalose-treated transgenic mice, AT100-positive tau aggregates were also immunoreactive for LC3, indicating the co-localization of autophagic vacuoles and tau aggregates (arrows, Fig. 1F–H).

Effects of trehalose on tau pathology and neuronal survival

Total soluble tau and soluble tau phosphorylated at the AT8 epitope were not affected by trehalose treatment (Supplementary Fig. 2). In contrast, quantification of sarkosyl-insoluble tau in the brain indicated that trehalose decreased the amount of insoluble tau compared with untreated controls (-53%, $P < 0.01$) or to controls treated with sucrose (-46%, $P < 0.05$) (Fig. 2A). Trehalose treatment had no effect on the amount of sarkosyl-insoluble tau in the spinal cord (Fig. 2B). Immunofluorescence staining for anti-tau antibody AT100 showed a drastic reduction in the number of positive cells in layers I–III of the cerebral cortex (-66.5% compared with untreated animals, $P < 0.01$; -80.1% compared with sucrose-treated mice, $P < 0.001$) (Fig. 2C–F) and in the brainstem, particularly the pontine nucleus

Figure 1 Conversion of LC3-I into LC3-II was assessed by western blotting in the spinal cord (**A**) and the brain (**B**) of mice transgenic for human P301S tau. LC3-II staining was only present in brain where autophagic vacuoles were observed in trehalose-treated mice (arrow in **E**). Autophagic vacuoles were not present in the brains of non-treated (**C**) or sucrose-treated (**D**) mice. (**F–H**) Confocal analysis indicated that AT100-positive tau inclusions (**F**) were also immunoreactive for LC3-II (**G**), suggesting the presence of tau inclusions in autophagic vacuoles in trehalose-treated transgenic mice (**H**). NT = no treatment; Su = sucrose-treated; Tr = trehalose-treated. Scale bar = 20 μm.

(-75% compared with untreated animals, $P < 0.001$; -58.6% compared with sucrose-treated mice, $P < 0.01$) (Fig. 2G–J). Nerve cell numbers were counted in layers I–III of the cerebral cortex and in the pontine nucleus. The number of neurons in layers I–III was higher in trehalose-treated P301S tau mice than in animals that received either no treatment ($+55.5\%$, $P < 0.05$) or were treated with sucrose ($+59.6\%$, $P < 0.05$) (Fig. 3A). The number of neurons in trehalose-treated mice and in untreated wild-type animals was not significantly different (Fig. 3A). In the pontine nucleus, the number of neurons increased in trehalose-treated animals compared with untreated ($+79.2\%$, $P < 0.01$) and sucrose-treated controls ($+61.6\%$, $P < 0.05$) (Fig. 3B). The number of NeuN-positive cells in the pontine nucleus was similar in trehalose-treated P301S tau mice and in wild-type controls (Fig. 3B).

Effects of trehalose on p62/SQSTM1

Immunohistochemistry revealed the co-localization of p62/SQSTM1 and AT100-positive tau aggregates in P301S tau transgenic mice (Fig. 4D–F), while no co-staining was observed in wild-type controls (Fig. 4A–C). We assessed the levels of p62/SQSTM1 in the brains of wild-type and transgenic P301S tau mice subjected to the different treatments. We observed a reduction in p62/SQSTM1 levels in mice treated with trehalose compared with mice that received either no treatment (-52.1%, $P < 0.05$) or sucrose (-46.7%, $P < 0.05$) (Fig. 4G). No significant difference was detected between wild-type controls and P301S tau transgenic mice (Fig. 4G).

Discussion

The assembly of normally soluble proteins into amyloid-like fibrils is a pathological hallmark of several neurodegenerative disorders, with tauopathies being the most common (Goedert *et al.*, 2010). Herein, we report on the effects of stimulation of autophagy on tau inclusions and nerve cell survival in a mouse line transgenic for human mutant P301S tau. Trehalose activated autophagy in the brain, as shown by the increased formation of LC3-II, and reduced
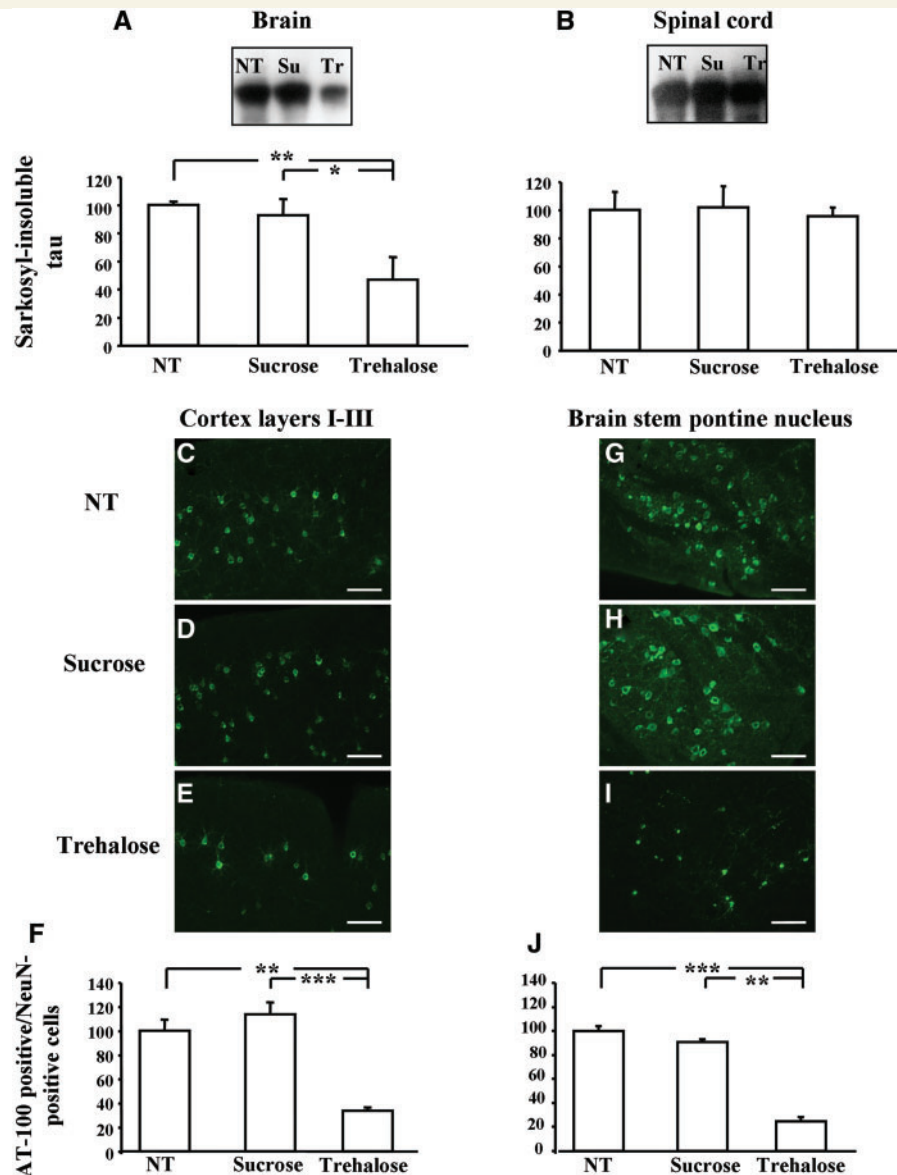
Figure 2 Sarkosyl-insoluble tau was decreased in the brain of trehalose-treated mice compared with non-treated or sucrose-treated animals (**A**), while trehalose treatment had no effect on sarkosyl-insoluble tau in the spinal cord (**B**). In trehalose-treated mice, the number of nerve cells with AT100-positive inclusions was drastically reduced in layers I–III of the cerebral cortex (**C–F**) and in the pontine nucleus of the brainstem (**G–J**). NT = no treatment; Su = sucrose-treated; Tr = trehalose-treated. $*P < 0.05$, $**P < 0.01$ and $***P < 0.001$.

the level of sarkosyl-insoluble tau. However, it did not stimulate autophagy in the spinal cord and consequently had no effect on the level of insoluble tau. The mechanism of action of trehalose is not completely understood, but it is believed to activate autophagy in an mTOR-independent manner (Sarkar *et al.*, 2007a). These findings suggest that autophagic pathways may differ between brain and spinal cord. The absence of a detectable effect of trehalose in the spinal cord probably accounted for the persistence of a pathological motor phenotype in treated P301S tau transgenic mice. We cannot exclude that a detailed behavioural assessment could have revealed subtle differences between treated and non-treated mice. However, the motor deficit characteristic of the human P301S tau transgenic mice probably results

from the degeneration of spinal cord motor neurons, consequent to the development of a toxic filamentous tau pathology (Allen *et al.*, 2002; Delobel *et al.*, 2008), and possibly the sequestration of proteins important for motor behaviour. As tau pathology in the spinal cord was unchanged after trehalose administration, an improvement in motor function was unlikely. The reasons underlying our inability to activate autophagy in the spinal cord remain to be determined. They could be related to a less efficient delivery of trehalose to the spinal cord, although it has been shown that the blood–spinal cord barrier is more permeable to tracers and cytokines than the blood–brain barrier (Prockop *et al.*, 1995; Pan *et al.*, 1997). We hope that future experiments will allow us to overcome this limitation.

A Cerebral cortex layers I–III

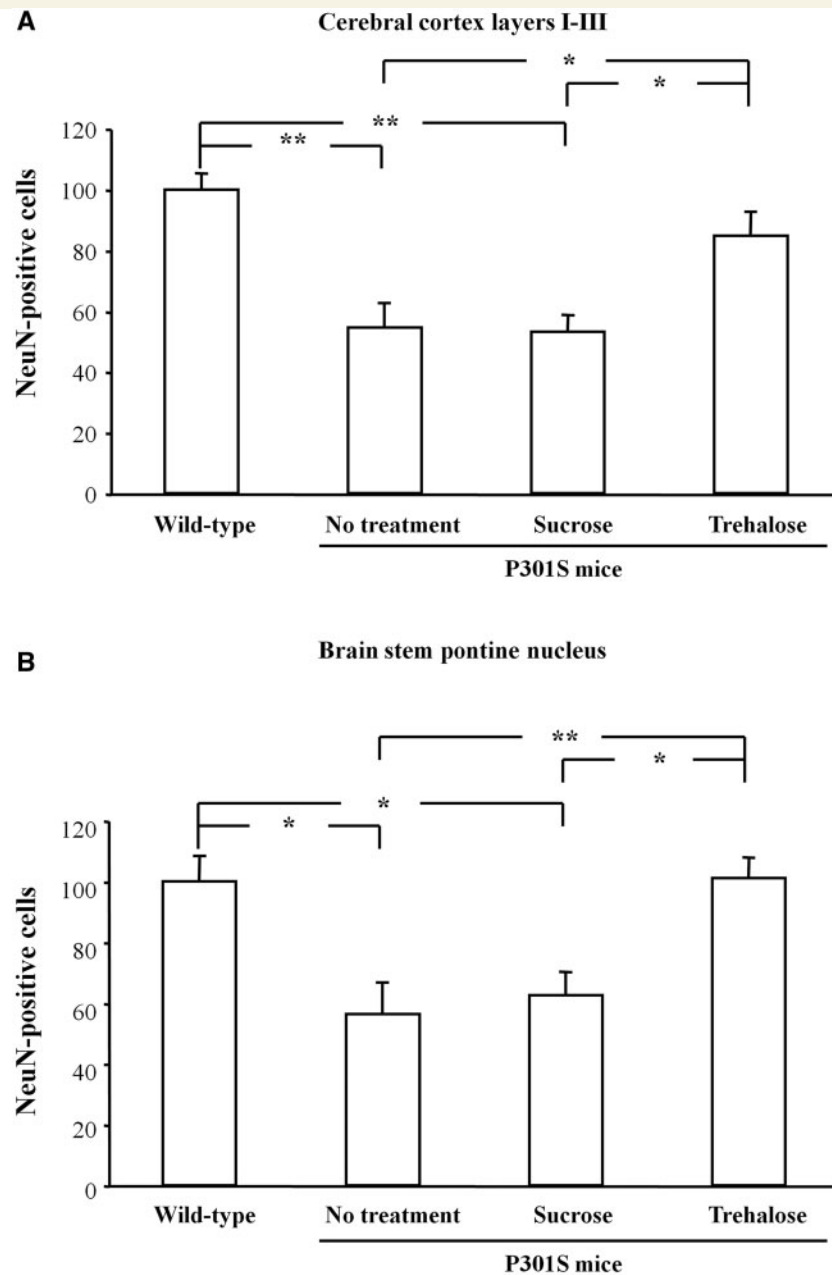**B** Brain stem pontine nucleus

Figure 3 Nerve cell numbers were assessed using stereology. Trehalose treatment increased the number of neurons in layers I–III of the cerebral cortex (**A**) and in the pontine nucleus of the brainstem (**B**). *$P < 0.05$ and **$P < 0.01$.

In the brains of trehalose-treated mice, we observed a decrease in sarkosyl-insoluble tau and the number of nerve cells with tau inclusions. Besides its ability to activate autophagy, trehalose has also been reported to act as a protective chaperone in a murine model of Huntington's disease (Tanaka *et al.*, 2004). However, the reduction in tau inclusions in our mouse line was probably due to the degradation of tau aggregates by trehalose-induced autophagy. Indeed, we observed a decrease in tau inclusions only in regions where autophagy was activated. Moreover, we showed co-localization between autophagic vacuoles and tau inclusions, suggesting that tau aggregates were engulfed by autophagosomes before degradation. Sucrose, a chemical

chaperone, which has been shown to reduce the conversion of the cellular prion protein to its protease-resistant form (DebBurman *et al.*, 1997), failed to reduce tau aggregates in the human mutant P301S tau transgenic mice, confirming that the effect of trehalose on tau aggregates was mediated through an increase in autophagy.

Altogether, our results indicate that the *in vivo* stimulation of autophagy reduced the amount of tau aggregates and improved nerve cell survival. A role for autophagy in the clearance of protein aggregates has been suggested for a number of proteins, including β-amyloid, α-synuclein, ataxin-3, prion protein and huntingtin (Webb *et al.*, 2003; Sarkar *et al.*, 2007b; Pickford *et al.*, 2008;
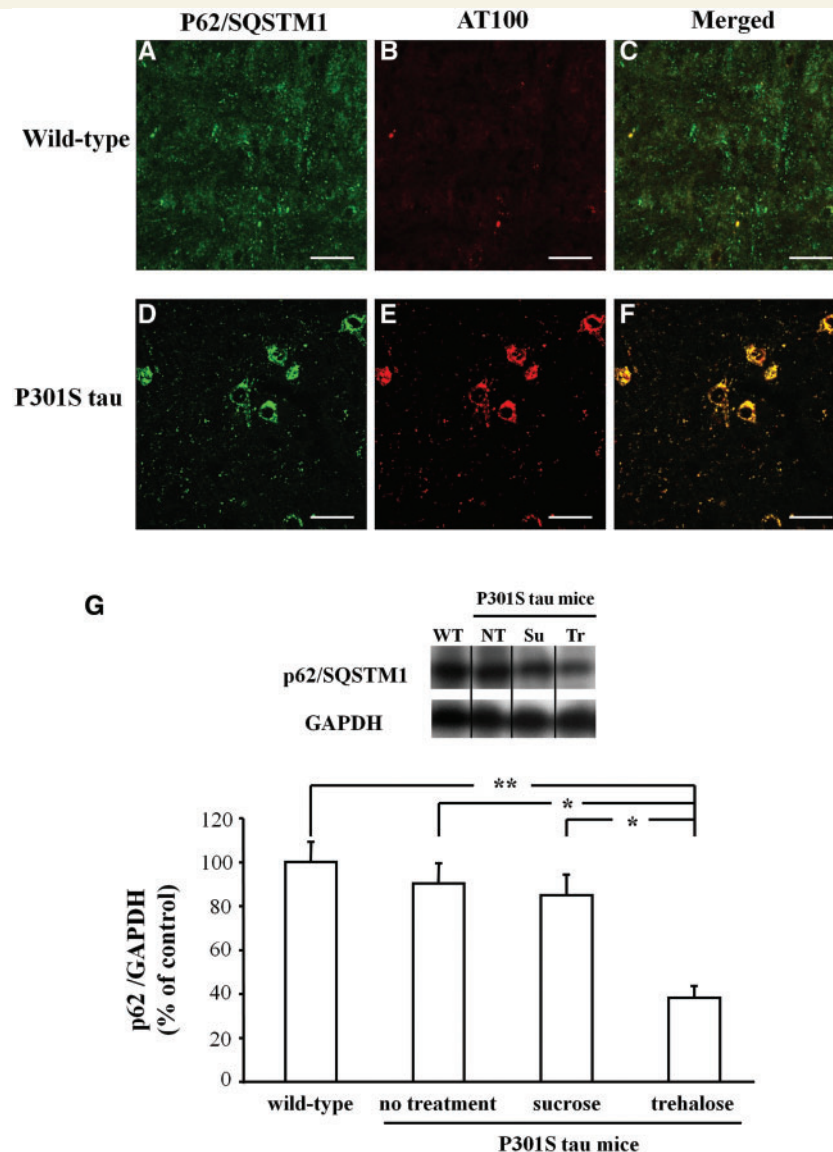
Figure 4 Immunohistochemistry for p62/SQSTM1 (**A** and **D**) and assembled tau (AT100; **B** and **E**) showed co-localization in P301S tau transgenic mice (**F**) but not in wild-type animals (**C**). Scale bar = 20 μm. (**G**) Western blot of p62/SQSTM1 levels in the brains of wild-type controls and mice transgenic for human mutant P301S tau that received either no treatment or were given sucrose or trehalose. The amount of p62/SQSTM1 signal is shown normalized with respect to GAPDH. *$P < 0.05$ and **$P < 0.01$.

Heiseke *et al.*, 2009; Casarejos *et al.*, 2011; Majumder *et al.*, 2011; Riedel *et al.*, 2011; Spilman *et al.*, 2011). Activation of autophagy has also shown protective effects in mouse and fly models of tauopathy (Berger *et al.*, 2006; Caccamo *et al.*, 2011; Majumder *et al.*, 2011; Rodriguez-Navarro *et al.*, 2011). However, in mice, tau was not the only engineered protein. In one study, the mice overexpressed human mutant tau and carried a deletion of the gene encoding parkin (Rodriguez-Navarro *et al.*, 2011), a potential mediator of autophagy (Olzmann *et al.*, 2007; Chin *et al.*, 2011). Therefore, not surprisingly, restoration of autophagic activity decreased the number of tau aggregates and improved cell survival. In separate studies, autophagy was activated in triple transgenic mice exhibiting tau and β-amyloid pathologies (Caccamo *et al.*, 2011; Majumder *et al.*, 2011). It is

well established that β-amyloid can promote tau pathology in some brain regions (Götz *et al.*, 2001; Lewis *et al.*, 2001; Oddo *et al.*, 2003, 2004). However, direct evidence for the relevance of autophagy in modulating tau pathology was missing. We now show that the activation of autophagy markedly reduced the number of tau aggregates and nerve cell loss in a mouse model of human tauopathy.

We also investigated p62/SQSTM1 expression in wild-type and P301S tau transgenic mice. p62/SQSTM1 is a protein that acts as a receptor for selective autophagy, mainly because of its ability to bind both ubiquitin and LC3 (Pankiv *et al.*, 2007; Lamark *et al.*, 2009). It has previously been implicated in the degradation of protein inclusions (Bjorkoy *et al.*, 2006; Watanabe and Tanaka, 2011) and has been found in tau inclusions in human

neurodegenerative diseases (Kuusisto *et al.*, 2001, 2002; Zatloukal *et al.*, 2002). We now show co-localization of p62/SQSTM1 with tau inclusions in P301S tau transgenic mice, consistent with the human pathology. In addition, we observed a decrease in p62/SQSTM1 levels in trehalose-treated mice, suggesting that p62/SQSTM1 may be an adaptor molecule for tau inclusions before their degradation by autophagy. Although the majority of tau filaments in P301S tau transgenic are not ubiquitinated (Allen *et al.*, 2002), p62/SQSTM1 may nonetheless be involved, as it has been shown to play a role in the autophagic degradation of non-ubiquitinated protein aggregates (Watanabe and Tanaka, 2011). The levels of p62/SQSTM1 were similar between P301S tau transgenic mice and wild-type controls, indicating that p62/SQSTM1 synthesis and basal autophagy were not affected in the transgenic mice. In conclusion, we show that activation of autophagy in mice transgenic for human mutant P301S tau decreased the number of tau inclusions and increased nerve cell survival in cerebral cortex and brainstem.

Acknowledgements

Funding

Supplementary material

Supplementary material is available at *Brain* online.

References

Allen B, Ingram E, Takao M, Smith MJ, Jakes R, Virdee K, et al. Abundant tau filaments and nonapoptotic neurodegeneration in transgenic mice expressing human P301S tau protein. J Neurosci 2002; 22: 9340–51.

Bedford L, Hay D, Devoy A, Paine S, Powe DG, Seth R, et al. Depletion of 26S proteasomes in mouse brain neurons causes neurodegeneration and Lewy-like inclusions resembling human pale bodies. J Neurosci 2008; 28: 8189–98.

Berger Z, Ravikumar B, Menzies FM, Oroz LG, Underwood BR, Pangalos MN, et al. Rapamycin alleviates toxicity of different aggregate-prone proteins. Hum Mol Genet 2006; 15: 433—42.

Bjorkoy G, Lamark T, Johansen T. p62/SQSTM1: a missing link between protein aggregates and the autophagy machinery. Autophagy 2006; 2: 138–9.

Blard O, Frebourg T, Campion D, Lecourtois M. Inhibition of proteasome and Shaggy/Glycogen synthase kinase-3β kinase prevents clearance of phosphorylated tau in *Drosophila*. J Neurosci Res 2006; 84: 1107–15.

Caccamo A, Majumder S, Richardson A, Strong R, Oddo S. Molecular interplay between mammalian target of rapamycin (mTOR), amyloid-β, and Tau: effects on cognitive impairments. J Biol Chem 2011; 285: 13107–20.

Casarejos MJ, Solano RM, Gomez A, Perucho J, de Yebenes JG, Mena MA. The accumulation of neurotoxic proteins, induced by proteasome inhibition, is reverted by trehalose, an enhancer of autophagy, in human neuroblastoma cells. Neurochem Int 2011; 58: 512–20.

Chin LS, Olzmann JA, Li L. Parkin-mediated ubiquitin signalling in aggresome formation and autophagy. Biochem Soc Trans 2011; 38: 144–9.

DebBurman SK, Raymond GJ, Caughey B, Lindquist S. Chaperone-supervised conversion of prion protein to its protease-resistant form. Proc Natl Acad Sci USA 1997; 94: 13938–43.

Delobel P, Lavenir I, Fraser G, Ingram E, Holzer M, Ghetti B, et al. Analysis of tau phosphorylation and truncation in a mouse model of human tauopathy. Am J Pathol 2008; 172: 123–31.

Giannakopoulos P, Herrmann FR, Bussiere T, Bouras C, Kovari E, Perl DP, et al. Tangle and neuron numbers, but not amyloid load, predict cognitive status in Alzheimer's disease. Neurology 2003; 60: 1495–500.

Goedert M, Clavaguera F, Tolnay M. The propagation of prion-like protein inclusions in neurodegenerative diseases. Trends Neurosci 2010; 33: 317–25.

Goedert M, Jakes R. Mutations causing neurodegenerative tauopathies. Biochim Biophys Acta 2005; 1739: 240–50.

Goedert M, Jakes R, Vanmechelen E. Monoclonal antibody AT8 recognises tau protein phosphorylated at both serine 202 and threonine 205. Neurosci Lett 1995; 189: 167–9.

Goedert M, Spillantini MG. Pathogenesis of the Tauopathies. J Mol Neurosci 2011; 45: 7.

Goldberg AL. Protein degradation and protection against misfolded or damaged proteins. Nature 2003; 426: 895–9.

Götz J, Chen F, van Dorpe J, Nitsch RM. Formation of neurofibrillary tangles in P301L tau transgenic mice induced by Abeta 42 fibrils. Science 2001; 293: 1491–5.

Hara T, Nakamura K, Matsui M, Yamamoto A, Nakahara Y, Suzuki-Migishima R, et al. Suppression of basal autophagy in neural cells causes neurodegenerative disease in mice. Nature 2006; 441: 885–9.

Heiseke A, Aguib Y, Riemer C, Baier M, Schatzl HM. Lithium induces clearance of protease resistant prion protein in prion-infected cells by induction of autophagy. J Neurochem 2009; 109: 25–34.

Kabeya Y, Mizushima N, Ueno T, Yamamoto A, Kirisako T, Noda T, et al. LC3, a mammalian homologue of yeast Apg8p, is localized in autophagosome membranes after processing. EMBO J 2000; 19: 5720–8.

Komatsu M, Waguri S, Chiba T, Murata S, Iwata J, Tanida I, et al. Loss of autophagy in the central nervous system causes neurodegeneration in mice. Nature 2006; 441: 880–4.

Kuusisto E, Salminen A, Alafuzoff I. Ubiquitin-binding protein p62 is present in neuronal and glial inclusions in human tauopathies and synucleinopathies. Neuroreport 2001; 12: 2085–90.

Kuusisto E, Salminen A, Alafuzoff I. Early accumulation of p62 in neurofibrillary tangles in Alzheimer's disease: possible role in tangle formation. Neuropathol Appl Neurobiol 2002; 28: 228–37.

Lamark T, Kirkin V, Dikic I, Johansen T. NBR1 and p62 as cargo receptors for selective autophagy of ubiquitinated targets. Cell Cycle 2009; 8: 1986–90.

Lee BH, Lee MJ, Park S, Oh DC, Elsasser S, Chen PC, et al. Enhancement of proteasome activity by a small-molecule inhibitor of USP14. Nature 2010; 467: 179–84.

Lewis J, Dickson DW, Lin WL, Chisholm L, Corral A, Jones G, et al. Enhanced neurofibrillary degeneration in transgenic mice expressing mutant tau and APP. Science 2001; 293: 1487–91.

Lin WL, Lewis J, Yen SH, Hutton M, Dickson DW. Ultrastructural neuronal pathology in transgenic mice expressing mutant (P301L) human tau. J Neurocytol 2003; 32: 1091–105.

Lind D, Franken S, Kappler J, Jankowski J, Schilling K. Characterization of the neuronal marker NeuN as a multiply phosphorylated antigen with discrete subcellular localization. J Neurosci Res 2005; 79: 295–302.

Liu YH, Wei W, Yin J, Liu GP, Wang Q, Cao FY, et al. Proteasome inhibition increases tau accumulation independent of phosphorylation. Neurobiol Aging 2009; 30: 1949–61.

Majumder S, Richardson A, Strong R, Oddo S. Inducing autophagy by rapamycin before, but not after, the formation of plaques and tangles ameliorates cognitive deficits. PLoS One 2011; 6: e25416.

Mizushima N, Yamamoto A, Matsui M, Yoshimori T, Ohsumi Y. In vivo analysis of autophagy in response to nutrient starvation using transgenic mice expressing a fluorescent autophagosome marker. Mol Biol Cell 2004; 15: 1101–11.

Mullen RJ, Buck CR, Smith AM. NeuN, a neuronal specific nuclear protein in vertebrates. Development 1992; 116: 201–11.

Nixon RA, Wegiel J, Kumar A, Yu WH, Peterhoff C, Cataldo A, et al. Extensive involvement of autophagy in Alzheimer disease: an immuno-electron microscopy study. J Neuropathol Exp Neurol 2005; 64: 113–22.

Noda T, Ohsumi Y. Tor, a phosphatidylinositol kinase homologue, controls autophagy in yeast. J Biol Chem 1998; 273: 3963–6.

Oddo S, Billings L, Kesslak JP, Cribbs DH, LaFerla FM. Aβ immuno-therapy leads to clearance of early, but not late, hyperphosphorylated tau aggregates via the proteasome. Neuron 2004; 43: 321–32.

Oddo S, Caccamo A, Kitazawa M, Tseng BP, LaFerla FM. Amyloid deposition precedes tangle formation in a triple transgenic model of Alzheimer's disease. Neurobiol Aging 2003; 24: 1063–70.

Olzmann JA, Li L, Chudaev MV, Chen J, Perez FA, Palmiter RD, et al. Parkin-mediated K63-linked polyubiquitination targets misfolded DJ-1 to aggresomes via binding to HDAC6. J Cell Biol 2007; 178: 1025–38.

Pan W, Banks WA, Kastin AJ. Permeability of the blood-brain and blood-spinal cord barriers to interferons. J Neuroimmunol 1997; 76: 105–11.

Pankiv S, Clausen TH, Lamark T, Brech A, Bruun JA, Outzen H, et al. p62/SQSTM1 binds directly to Atg8/LC3 to facilitate degradation of ubiquitinated protein aggregates by autophagy. J Biol Chem 2007; 282: 24131–45.

Pickford F, Masliah E, Britschgi M, Lucin K, Narasimhan R, Jaeger PA, et al. The autophagy-related protein beclin 1 shows reduced expression in early Alzheimer disease and regulates amyloid beta accumulation in mice. J Clin Invest 2008; 118: 2190–9.

Prockop LD, Naidu KA, Binard JE, Ransohoff J. Selective permeability of [³H]-D-mannitol and [¹⁴C]-carboxyl-inulin across the blood-brain barrier and blood-spinal cord barrier in the rabbit. J Spinal Cord Med 1995; 18: 221–6.

Ramesh Babu J, Lamar Seibenhener M, Peng J, Strom AL, Kemppainen R, Cox N, et al. Genetic inactivation of p62 leads to accumulation of hyperphosphorylated tau and neurodegeneration. J Neurochem 2008; 106: 107–20.

Riedel M, Goldbaum O, Schwarz L, Schmitt S, Richter-Landsberg C. 17-AAG induces cytoplasmic α-synuclein aggregate clearance by induction of autophagy. PLoS One 2011; 5: e8753.

Riley BE, Kaiser SE, Shaler TA, Ng AC, Hara T, Hipp MS, et al. Ubiquitin accumulation in autophagy-deficient mice is dependent on the Nrf2-mediated stress response pathway: a potential role for protein aggregation in autophagic substrate selection. J Cell Biol 2010; 191: 537–52.

Rodriguez-Navarro JA, Rodriguez L, Casarejos MJ, Solano RM, Gomez A, Perucho J, et al. Trehalose ameliorates dopaminergic and tau pathology in parkin deleted/tau overexpressing mice through autophagy activation. Neurobiol Dis 2011; 39: 423–38.

Sarkar S, Davies JE, Huang Z, Tunnacliffe A, Rubinsztein DC. Trehalose, a novel mTOR-independent autophagy enhancer, accelerates the clearance of mutant huntingtin and α-synuclein. J Biol Chem 2007a; 282: 5641–52.

Sarkar S, Perlstein EO, Imarisio S, Pineau S, Cordenier A, Maglathlin RL, et al. Small molecules enhance autophagy and reduce toxicity in Huntington's disease models. Nat Chem Biol 2007b; 3: 331–8.

Scattoni ML, Gasparini L, Alleva E, Goedert M, Calamandrei G, Spillantini MG. Early behavioural markers of disease in P301S tau transgenic mice. Behav Brain Res 2010; 208: 250–7.

Spilman P, Podlutskaya N, Hart MJ, Debnath J, Gorostiza O, Bredesen D, et al. Inhibition of mTOR by rapamycin abolishes cognitive deficits and reduces amyloid-beta levels in a mouse model of Alzheimer's disease. PLoS One 2011; 5: e9979.

Tanaka M, Machida Y, Niu S, Ikeda T, Jana NR, Doi H, et al. Trehalose alleviates polyglutamine-mediated pathology in a mouse model of Huntington disease. Nat Med 2004; 10: 148–54.

Tanida I, Ueno T, Kominami E. LC3 conjugation system in mammalian autophagy. Int J Biochem Cell Biol 2004; 36: 2503–18.

Watanabe Y, Tanaka M. p62/SQSTM1 in autophagic clearance of a non-ubiquitylated substrate. J Cell Sci 2011; 124: 2692–701.

Webb JL, Ravikumar B, Atkins J, Skepper JN, Rubinsztein DC. α-Synuclein is degraded by both autophagy and the proteasome. J Biol Chem 2003; 278: 25009–13.

Wolf HK, Buslei R, Schmidt-Kastner R, Schmidt-Kastner PK, Pietsch T, Wiestler OD, et al. NeuN: a useful neuronal marker for diagnostic histopathology. J Histochem Cytochem 1996; 44: 1167–71.

Yoshida H, Goedert M. Sequential phosphorylation of tau protein by cAMP-dependent protein kinase and SAPK4/p38δ or JNK2 in the presence of heparin generates the AT100 epitope. J Neurochem 2006; 99: 154–64.

Zatloukal K, Stumptner C, Fuchsbichler A, Heid H, Schnoelzer M, Kenner L, et al. p62 is a common component of cytoplasmic inclusions in protein aggregation diseases. Am J Pathol 2002; 160: 255–63.